Desalination and Water Treatment
www.deswater.com

doi: 10.5004/dwt.2020.25226

182 (2020) 320–331
April

Carboxyl functionalized hyper-cross-linked dendrimers and their adsorption of aniline from aqueous solution

Xiaomei Wang[a,*], Xiaomi Yuan[b], Fa Zhou[b], Jianhan Huang[b]

[a]*College of Biology and Environmental Engineering, Changsha University, Changsha 410003, China, email: wxm11@ccsu.edu.cn (X. Wang)*
[b]*College of Chemistry and Chemical Engineering, Central South University, Changsha 410083, China, emails: 857122353@qq.com (X. Yuan), 605916930@qq.com (F. Zhou), jianhanhuang@csu.edu.cn (J. Huang)*

Received 18 July 2019; Accepted 20 November 2019

ABSTRACT

Functionalized hyper-cross-linked polymers with special functional groups are anticipated for fast and efficient removal of aniline from aqueous solution. Herein, sequential four chemical reactions namely polymerization, Friedel–Crafts reaction, amination reaction, and carboxylation reaction were performed and carboxyl functionalized hyper-cross-linked dendrimers with highly branched structure and multiple functional groups were fabricated. The introduced carboxyl, amino, and amido groups on the polymers exhibit strong affinity to aniline through acid-base interaction, electrostatic interaction, and hydrogen bonding, which are helpful for the equilibrium adsorption of aniline. Importantly, these polymers owned hierarchical microporous and mesoporous structure, which is beneficial for the fast adsorption of aniline. These polymers were efficient for aniline adsorption with a maximum capacity of 163.0 mg/g and the adsorption was an exothermic, spontaneous, and ordered process. The adsorption was a fast process and less than 10 min was required to reach the equilibrium. The present study gives a simple strategy for the synthesis of carboxyl functionalized hyper-cross-linked dendrimers, which is of great significance for the fast and efficient adsorption of aniline from aqueous solution.

Keywords: Carboxyl; Dendrimers; Adsorption; Aniline

1. Introduction

Aniline is one of the most crucial intermediates for the production of dyes, drugs, explosives, and plastics [1]. Nevertheless, aniline is a common pollutant in the environment, it is greatly harmful to humans even at a very low concentration [2]. It has strong toxicity to blood and nerves, and chronic exposure of aniline may also result in bad effects on the blood. Animal studies have proven that aniline can cause spleen tumors. As a result, fast and efficient removal of aniline from aqueous solution has become a hot topic in recent years [3–6].

Adsorption by solid adsorbents is proven to be simple while efficient for the removal of aniline from aqueous solution. Due to their high Brunauer–Emmett–Teller (BET) surface area (S_{BET}) and outstanding porosity, hyper-cross-linked polymers (HCPs) are efficient for adsorptive removal of aniline from aqueous solution [7,8]. In particular, some special functional groups such as the carboxyl (–COOH), amino (–NH_2/–NH–), and hydroxyl (–OH) are embedded in

* Corresponding author.

the HCPs by polar monomers or post chemical modification [9–12]. Thus, the functionalized HCPs have increased equilibrium capacity (q_e) to aniline due to the introduced chemical interactions including acid-base interaction, electrostatic interaction, and hydrogen bonding.

Notably, the polymers with dendritic structure have diversified functional groups on the branches, the highly repeated units of the functional groups offer multiple chemical interactions between the dendrimers and the adsorbates, endowing them with not only excellent physical characteristics but also admirable performance [13–15], and they are mainly used as adsorbents to remove organic pollutants and heavy metals in aqueous solution [16,17], biomedical macromolecules [18,19], targeting drug carriers [20], catalysts [21], and sensors [22]. For example, Golikand et al. [23] synthesized a triazine-based dendrimer with a poly(ethylene glycol) core. It is found that the introduced heteratoms such as nitrogen (N) and oxygen (O) are beneficial for the chelating of Cu^{2+}, Ni^{2+}, and Zn^{2+}. Niu et al. [24] used polyamide-amine (PAMAM) dendrimers to adsorb Hg^{2+}, the adsorption mechanism proposed that the repeated units of the amido (–CONH–) and amino (–NH_2/–NH–) groups make Hg^{2+} adsorption much enhanced due to the strong chelating. If the strategy for the synthesis of the dendrimers can be employed for the HCPs, the combination of high S_{BET}, outstanding porosity, and highly repeated functional groups will make the newly prepared hyper-cross-linked dendrimers better adsorption to aniline. Our previous work has shown that the dendritic post-cross-linked resins are efficient for adsorption of crystal violet from aqueous solution [25], and the carboxyl, amino, and amido groups on the dendrimers play a positive role.

Herein, p-vinylbenzyl chloride (VBC) and ethylene glycol dimethacrylate (EGDMA) were employed as the monomers for the production of the HCPs. Afterward, two sequential functionalized reactions namely amination and carboxylation were performed for the HCPs, and thus the carboxyl functionalized hyper-cross-linked dendrimers were fabricated. These polymers have both advantages of the HCPs and the dendrimers. As for the HCPs, they have relatively high S_{BET} with hierarchical microporous and mesoporous distribution. As the dendrimers, they have considerable carboxyl, amino, and amido groups. These two merits of the resulting polymers endow them with much enhanced adsorptive removal of aniline. As compared to some other adsorbents such as acid modified activated carbon [26,27], inorganically modified mesoporous silica [28], and activated kaolinite [29,30].

2. Materials and methods

2.1. Materials

VBC (purity: 98%) and ethylene glycol dimethylacrylate (EGDMA) (purity: >99%) purchased from Chengdu West Asia Chemical Co. Ltd., China was extracted with 5% NaOH aqueous solution and deionized water until the solution was neutral. After that, they were dried with anhydrous $MgSO_4$ and placed in the refrigerator overnight before use. 1,2,4,5-benzenetetracarboxylic (purity: >98%) acid was purchased from Aladdin Reagent (USA) and used directly. 1,2-dichloroethane (DCE), anhydrous $FeCl_3$, and diethylenetriamine (DETA) were analytical reagents and used without further purification.

2.2. Preparation of carboxyl functionalized hyper-cross-linked dendrimers

Fig. 1 details the reaction process for the synthesis of carboxyl functionalized hyper-cross-linked dendrimers. Specifically, 180 mL of deionized water and 20 mL of 1% (w/w) aqueous solution of polyvinyl alcohol were uniformly mixed in a 500 mL flask with three necks, 40 g of toluene was used as solvent and 20 g of EGDMA and VBC were added, wherein EGDMA was the cross-linking agent and VBC was the monomer, and the cross-linking degree (the feeding amount of EGDMA) was controlled to be 10%, 20%, and 40%, respectively. The reaction was controlled to react at 358 K for 12 h, and hence the precursor polymers called X%-PVE (where X represents the initial cross-linking degree of the polymer) were synthesized.

The obtained precursor polymers were swollen with DCE overnight. Then, the Friedel–Crafts reaction was carried out for 12 h under anhydrous $FeCl_3$ as the catalyst 363 K, the produced hyper-cross-linked polymers named X%-HPE. Subsequently, DETA was used as the aminating agent and solvent, the amination reaction was carried out at 408 K and maintained for 12 h, the aminated functionalized hyper-cross-linked polymers were called X%-PED.

The aminated functionalized hyper-cross-linked polymers were swollen overnight with DMSO, superfluous pyromellitic acid was added into the reaction mixture. After the dissolution was completed, the temperature of the reaction mixture raised to 433 K. The reaction was carried out for 12 h,

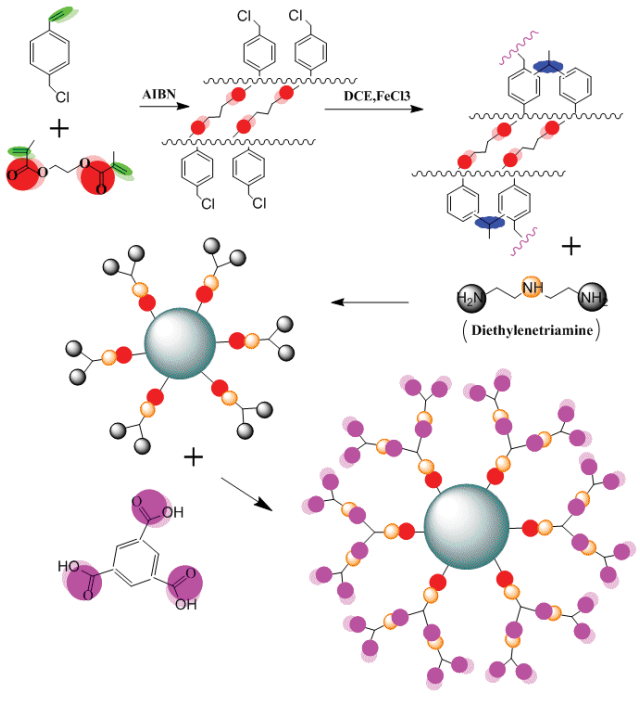

Fig. 1. The synthetic procedure of 20%-PEDPa.

and hence gained the carboxyl functionalized hyper-cross-linked dendrimers called X%-PEDPa.

2.3. Characterization

A Nicolet 510P (USA) Fourier transform infrared spectrometer was employed to record the Fourier transform infrared spectroscopy (FT-IR) of the samples. The specific surface area and pore structure parameters of the polymers were determined by N_2 adsorption-desorption isotherm on the Micromeritics ASAP 2020 (USA) surface area and porosity analyzer. The chlorine content of the polymers was measured according to the Volhard method. The X-ray photoelectron spectroscopy (XPS) was collected on a Thermo ESCALAB 250 spectrometer (USA) using an Al Ka X-ray source. The scanning electron microscopy (SEM, PW-100-011, Netherlands) was used to detect the morphology. The sample was pressed into a sheet of about 2 mm by a manual tableting machine and then placed in a contact angle measuring instrument (CA, JC 20 0 0D1, China) to measure the contact angle of the polymers. The thermogravimetric analysis (TGA) of the samples was investigated by a thermobalance (STA-499C, NETZSCH, USA). The concentration of aniline was measured via a UV-2450 spectrophotometer (Shimadzu Coop., Nakagyo-ku, Kyoto, Japan).

2.4. Adsorption experiments

The equilibrium isotherm of aniline adsorption on the polymers was carried out at 303 and 313 K. 0.1 g of the polymers and 50 mL of aniline aqueous solution with the initial concentration of about 100, 200, 300, 400, and 500 mg/L were mixed. The conical flasks were placed in a water bath shaker under the designed temperature for 4 h to reach the equilibrium. The residual aniline aqueous solution was separated and the equilibrium concentration of aniline was determined. The equilibrium capacity q_e (mg/g) was calculated as

$$q_e = \frac{\left(C_0 - C_e\right)V}{M} \tag{1}$$

where V is the volume of the solution (L) and M is the mass of the polymers (g).

In the kinetic adsorption, 0.5 g of the polymers and 250 mL of aniline aqueous solution at an initial concentration of 502.9 mg/L were mixed. The kinetic adsorption was measured at 303, 313, and 323 K, respectively. 0.5 mL of the aniline aqueous solution was taken in the adsorption and it was diluted a certain multiple at a certain time interval, the concentration of aniline C_t (mg/L) was measured at the given time t (min) and the adsorption capacity q_t (mg/g) of the aniline at time t is determined as,

$$q_t = \frac{\left(C_0 - C_t\right)V}{M} \tag{2}$$

3. Results and discussion

3.1. Structural characterization

The FT-IR of the precursor copolymers 10%-PVE, 20%-PVE, and 40%-PVE has the band at 1,724 cm^{-1} and this band is related to the C=O stretching of EGDMA (Fig. 2) [26], the vibrations at 1,260 and 669 cm^{-1} can be assigned to the C–Cl stretching of VBC, as depicted in Scheme 1 [9]. Notably, a higher feeding amount of EGDMA (a higher initial cross-linking degree) results in a strengthened intensity of C=O stretching while weakened C–Cl stretching. That is, 40%-PVE owns the highest C=O stretching intensity while 10%-PVE has the greatest C–Cl stretching. The chlorine content of the precursors gives similar results (Table 1) [26]. 10%-PVE, 20%-PVE, and 40%-PVE have gradually decreased chlorine contents with the values of 14.43, 13.32, and 9.94 wt.%, respectively. Noticeably, the contact angles (CA) of the precursors are measured to be 102°, 90°, and 68.5°, respectively (Fig. 3 and Table 2), confirming the highest hydrophobicity of 10%-PVE while the greatest hydrophilicity of 40%-PVE.

The Friedel–Crafts reaction induces almost disappearance of the C–Cl stretching (Fig. 2) [25,26], and the chlorine content sharply decreases from 13.32 (20%-PVE) to 0.71 wt.% (20%-HPE) (Table 3). The other two precursors have similar phenomena, Table 1 shows that the chlorine contents decrease to 0.78 and 0.52 wt.% (10%-HPE and 40%-HPE). In addition, 20%-HPE has a much higher CA of 119° as compared to the precursor because plentiful methylene cross-linking bridges are produced in the polymer chains. Meanwhile, the amination of 20%-HPE by DETA causes the ester carbonyl to be red-shifted from 1,724 to 1,650 cm^{-1} [26,31,32], the ester groups have been transformed into amido groups. Additionally, a broad peak shows at 3,436 cm^{-1} due to the introduction of the $–NH_2$/–NH– groups [33]. The CA of 20%-PED is sharply decreased to 43° (Fig. 3), demonstrating the successful chemical modification of the polymers. After the carboxylation of 20%-PED, the band intensity at 1,724 cm^{-1} is strengthened [26,34] and another acylamino carbonyl at 1,666 cm^{-1} is shown for 20%-PEDPa. Similar phenomena are observed for 10%-PEDPa and 40%-PEDPa.

Elemental analysis (EA) shows that 20%-PEDPa contains 80.06 wt.% of carbon (C), 4.38 wt.% of N, and 5.02 wt.% of hydrogen (H), hence O can be calculated to be about 9.55 wt.%. The XPS in Fig. 4a reveals that the polymer has rich N and O. The C1s, N1s, and O1s are existent with the characteristic peaks at 285.2, 400.2, and 533.1 eV, respectively. In the high-resolution O1s (Fig. 4b), three peaks present at 531.8, 532.8, and 533.6 eV, corresponding to C=O, C–OH, and O=C–O, respectively [33,35]. The high-resolution N1s in Fig. 4c is distributed to O=C–NH and O=C–N vibrations at 400 and 410.86 eV, respectively [36,37].

TGA of 20%-PEDPa (Fig. 5) shows that it starts to lose weight at around 400°C, illustrating its good thermal stability. The covalent linkages and the presence of heat resistant amido groups and aromatic units should give a positive contribution [38]. The SEM images of the precursor in Fig. 6 indicate its very rough surface with sags and crests, this rough surface is smoother after the Friedel–Crafts reaction due to the produced methylene cross-linking bridges. The amination and carboxylation reaction makes the surface irregular again due to the uploaded functional groups such as the carboxyl, amino, and amido groups.

The porosity of the polymers was tested by N_2 adsorption–desorption isotherms (Fig. 7a) and the porous parameters are summarized in Table 3. The S_{BET} and total pore

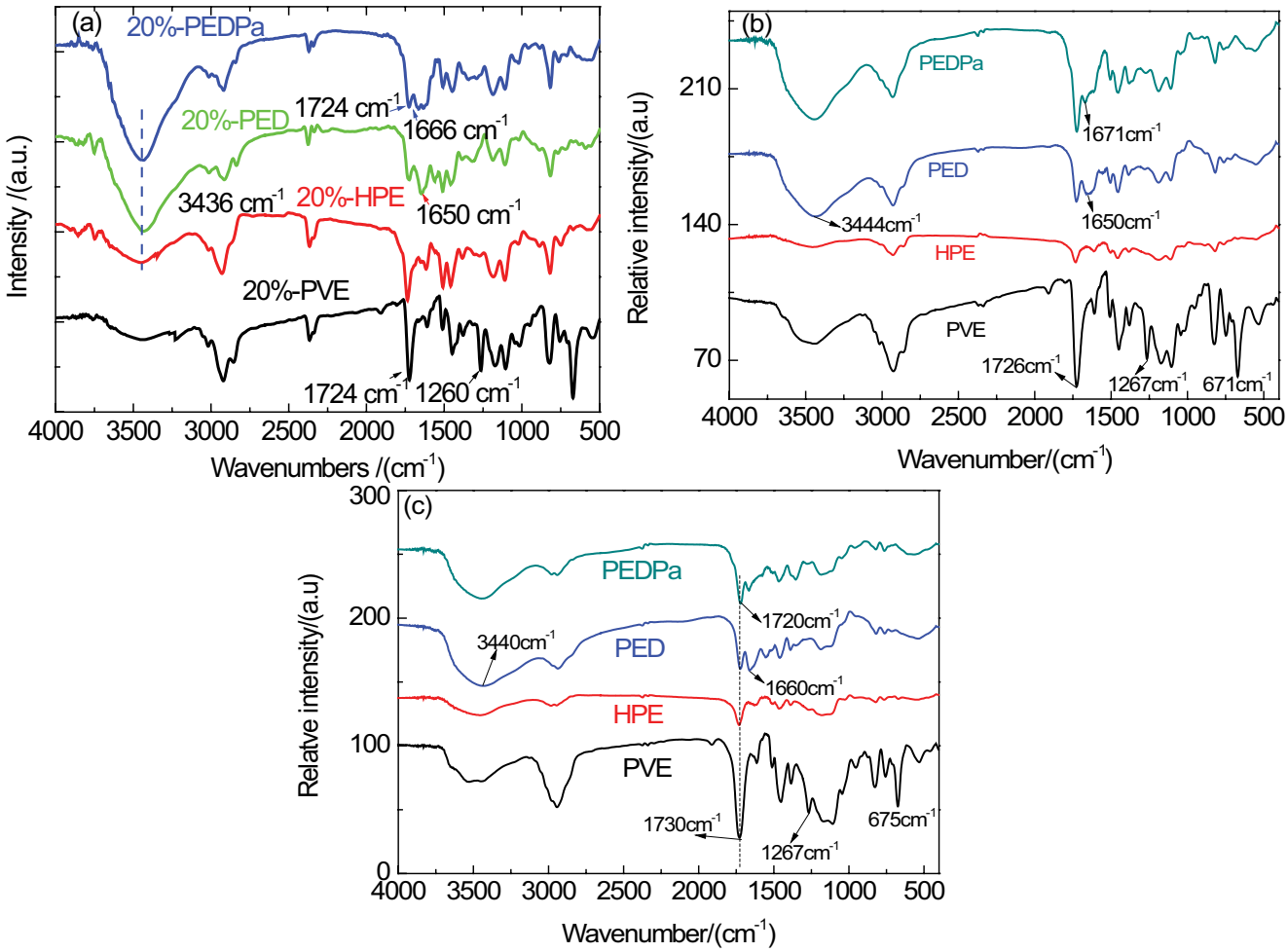

Fig. 2. FT-IR spectra of (a) 20%-PVE, 20%-HPE, 20%-PED, and 20%-PEDPa; (b) 10%-PVE, 10%-HPE, 10%-PED, and 10%-PEDPa; and (c) 40%-PVE, 40%-HPE, 40%-PED, and 40%-PEDPa.

Table 1
The chlorine content of 10%-PVE and 10%-HPE, 20%-PVE and 20%-HPE, and 40%-PVE and 40%-HPE

	10%-PVE	10%-HPE	20%-PVE	20%-HPE	40%-PVE	40%-HPE
Chlorine content (%)	14.43	0.78	13.32	0.71	9.94	0.52

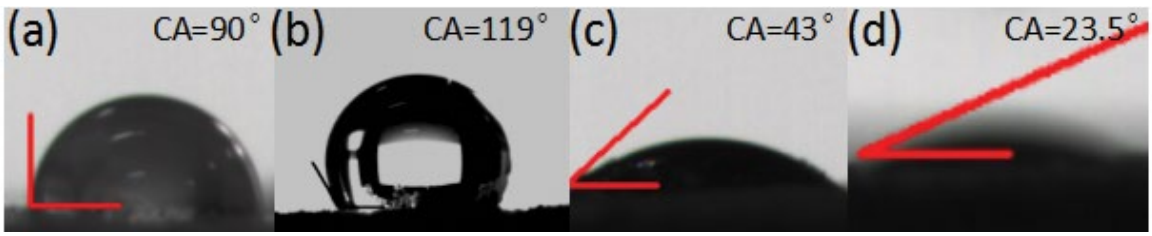

Fig. 3. Contact angles of (a) 20%-PVE, (b) 20%-HPE, (c) 20%-PED, and (d) 20%-PEDPa.

volume (V_{total}) of 20%-PVE are very low with the values of 16.8 m^2/g and 0.06 cm^3/g, respectively. After the Friedel–Crafts reaction, the S_{BET} (860 m^2/g) and V_{total} (1.0 $cm^3/$) of the polymer significantly increase attributed to the formation of a rigid methylene bridge [39]. In particular, the micropore area (S_{micro}) and micropore volume (V_{micro}) of 20%-HPE are 240 m^2/g and 0.13 cm^3/g, respectively. Based on the non-local density functional theory method, the pore size distribution

Table 2
The contact angle of 10%-PVE, 20%-PVE, and 40%-PVE

	10%-PVE	20%-PVE	40%-PVE
Contact angle/(°)	102	90	68.5

(PSD) of the polymers in Fig. 7b also displays that a large number of micropores and narrower mesopores in the range of 1–5 nm are produced in addition to the large mesopores (15–35 nm). On the contrary, the amination and carboxylation reaction make the S_{BET} and V_{total} gradually decrease to 694 m^2/g and 0.87 cm^3/g (20%-PED), and 674 m^2/g and

Table 3
Structural parameters of 20%-PVE, 20%-HPE, 20%-PED, and 20%-PEDPa, 10%-PEDPa, and 40%-PEDPa

	20%-PVE	20%-HPE	20%-PED	20%-PEDPa	10%-PEDPa	40%-PEDPa
$S_{BET}/(m^2/g)^a$	16.8	860	694	674	859	243
$S_{micro}/(m^2/g)^b$	0	240	244	193	195	1.3
$V_{total}/(cm^3/g)^c$	0.06	1.0	0.87	0.85	0.62	0.88
$V_{micro}/(cm^3/g)^b$	0	0.13	0.13	0.10	0.10	0
Chlorine content/(wt.%)	13.32	0.71	0.55	0.52	0.52	0.48
Contact angle/(°)	90	119	43	23.5	48	-

[a]Calculated using the Brunauer–Emmett–Teller (BET) model.
[b]Calculated using a non-local density functional theory model.
[c]Calculated at $P/P_0 = 0.99$.

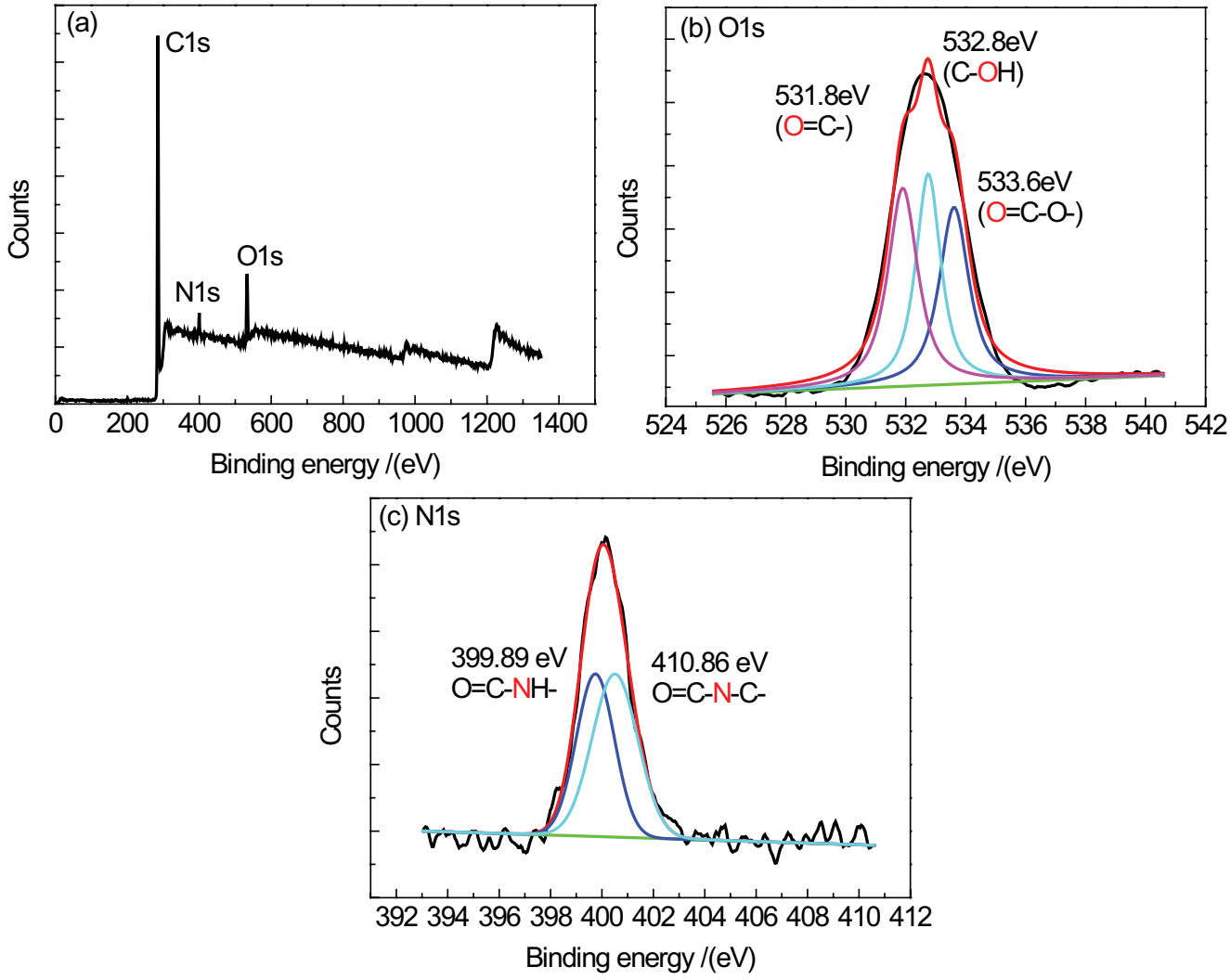

Fig. 4. XPS spectra of 20%-PEDPa (a) survey, (b) O1s, and (c) N1s.

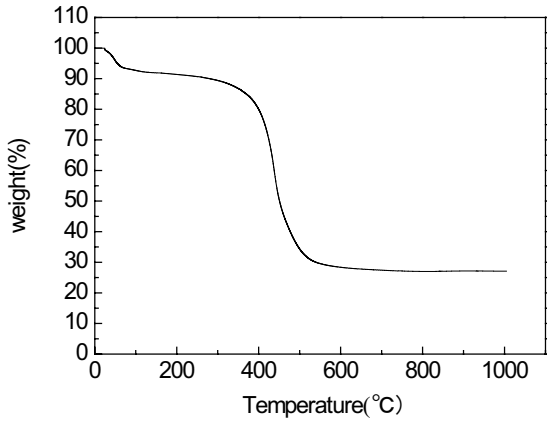

Fig. 5. TGA of 20%-PEDPa.

0.85 cm^3/g (20%-PEDPa). The ring cleavage of EGDMA and the elongation of the chain structure of the polymer should be the main reason. In addition, Fig. 8a means that increasing the initial cross-linking degree makes the S_{BET} decreased with the values of 859 m^2/g for 10%-PEDPa, 674 m^2/g for 20%-PEDPa, and 213 m^2/g for 40%-PEDPa. Particularly interesting, the V_{total} has an opposite order, which is increased from 0.62 to 0.85 and 0.88 cm^3/g. Moreover, the PSD has an obvious migration from the microporous and mesoporous region to mesoporous region as the initial cross-linking degree increases (Fig. 8b), this phenomenon is accordant with our previous finding [26].

3.2. Equilibrium adsorption

Fig. 9a compares the equilibrium isotherms of aniline adsorption on 20%-PVE, 20%-HPE, 20%-PED, and 20%-PEDPa at 303 K. The adsorption is greatly enhanced as the chemical reactions proceed and 20%-PEDPa has the best adsorption of aniline. 20%-PEDPa owns the lowest porous parameters such as the S_{BET} and V_{total}, while the uploaded carboxyl, amino, and amido groups can interact with aniline through several chemical interactions such as acid-base interaction, electrostatic interaction, and hydrogen bonding, which makes the adsorption enhanced. In addition, it is seen that the morphology of the polymers is in a colloidal scale with several hundred nanometers, whereas the dendrimers are on a molecular scale with several nanometers, and hence it can be concluded that the composition and morphology of the polymers are more important in the

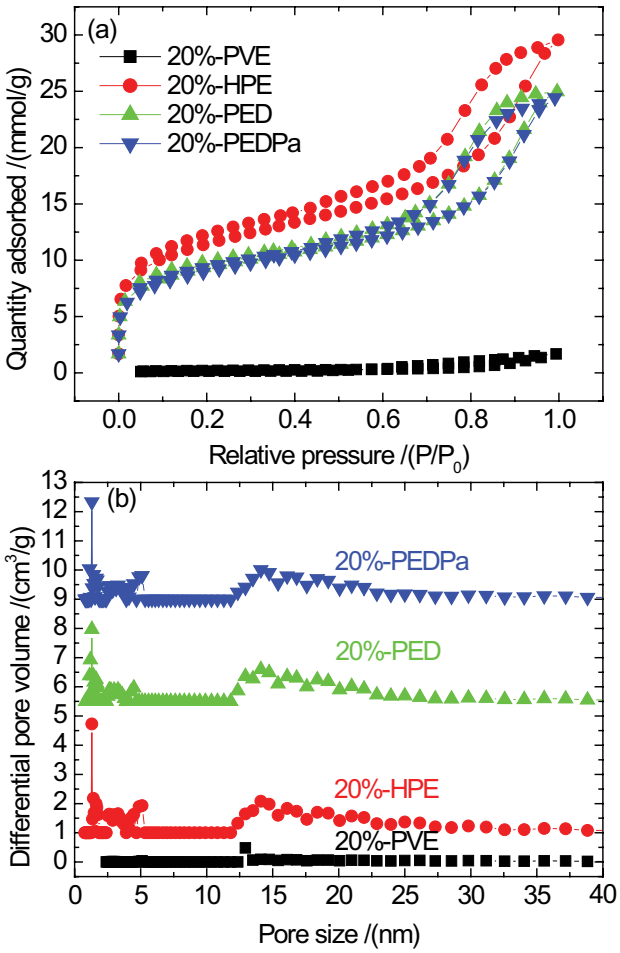

Fig. 7. (a) N_2 adsorption-desorption isotherms and (b) pore size distribution of 20%-PVE, 20%-HPE, 20%-PED, and 20%-PEDPa.

adsorption. The Langmuir and Freundlich models were used to describe the equilibrium data [40,41] and the fitted results are listed in Table 4. It can be concluded that these two models fit the equilibrium data well due to the high correlation coefficient ($R^2 > 0.98$). The maximum capacity (q_{max}) of 20%-HPE, 20%-PED, and 20%-PEDPa according to the Langmuir model were predicted to be 25.3, 143.5, 151.0, and 163.0 mg/g, respectively. A further comparison of the equilibrium isotherms of aniline on 10%-PEDPa, 20%-PEDPa, and 40%-PEDPa reveals that 20%-PEDPa has the largest q_{max} (Fig. 9b), indicating that the porous parameters

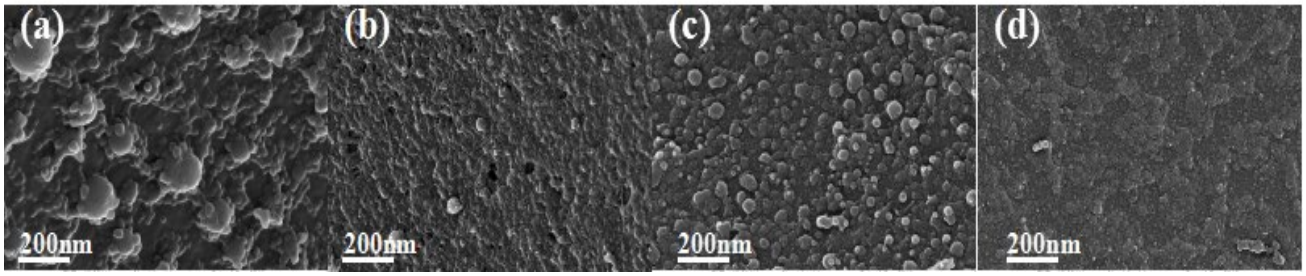

Fig. 6. SEM images of (a) 20%-PVE, (b) 20%-HPE, (c) 20%-PED, and (d) 20%-PEDPa.

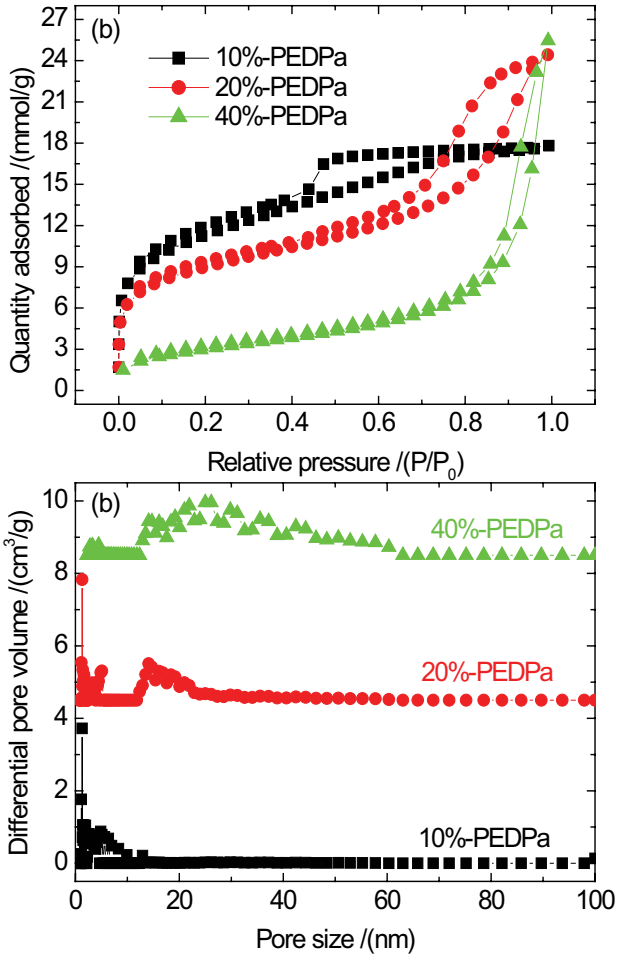

Fig. 8. (a) N_2 adsorption-desorption isotherms and (b) pore size distribution of 10%-PVE, 20%-HPE, 20%-PED, and 40%-PEDPa.

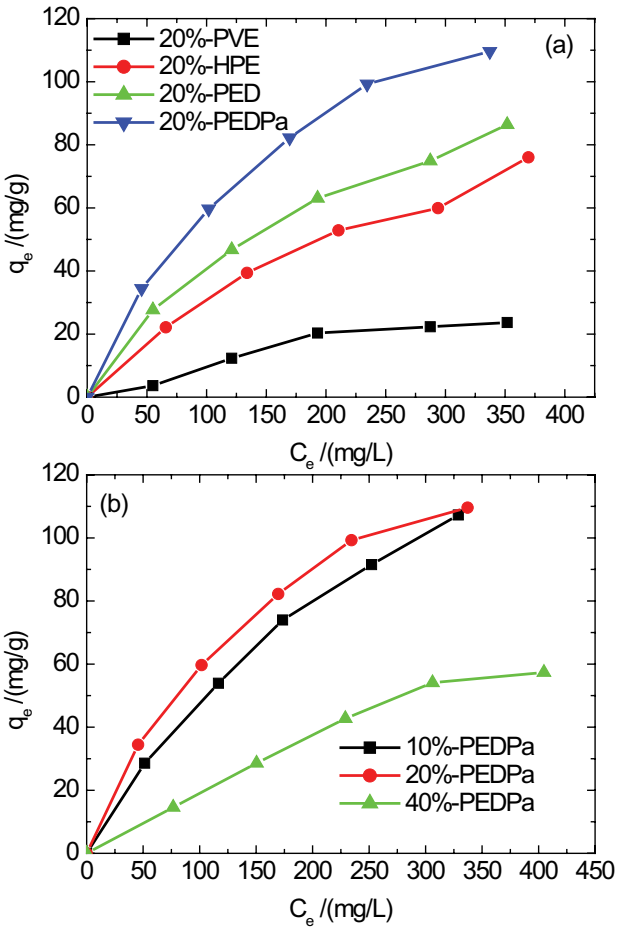

Fig. 9. Equilibrium isotherms of aniline adsorption on (a) 20%-HPE, 20%-PED, and 20%-PEDPa at 303 K and (b) 10%-PEDPa, 20%-PEDPa, and 40%-PEDPa at 303 K.

Table 4
Fitted parameters for the equilibrium data of aniline adsorption on 20%-HPE, 20%-PED, and 20%-PEDPa by the Langmuir and Freundlich models

	Langmuir model			Freundlich model		
	K_L (L/g)	q_m (mg/g)	R^2	K_F ((mg/g)(L/mg)$^{1/n}$)	n	R^2
20%-PVE	1.025×10^{-3}	23.50	0.9845	0.574	1.036	0.9952
20%-HPE	4.102×10^{-3}	143.5	0.9870	2.805	1.711	0.9973
20%-PED	2.525×10^{-3}	151.0	0.9897	1.447	1.501	0.9915
20%-PEDPa	3.322×10^{-3}	163.0	0.9913	2.583	1.659	0.9981
10%-PEDPa	2.801×10^{-3}	223.2	0.9895	2.182	1.482	0.9969
40%-PEDPa	1.787×10^{-3}	148.8	0.9852	0.7116	1.347	0.9950

are also decisive factors in the adsorption in addition to the introduced carboxyl, amino, and amido groups on the polymers. Moreover, the q_{max} of 20%-PEDPa is comparable or superior to most of the reported data in the literature (Table 5) [28–30,42–44]. In particular, the polymers developed in this paper have both advantages of the HCPs and the dendrimers. They have relatively high S_{BET} with hierarchical microporous and mesoporous distribution. They also possess considerable carboxyl, amino, and amido groups. These two merits endow them with much enhanced adsorptive removal of aniline.

The effect of the temperature on the adsorption was thereafter studied for 20%-PEDPa with the temperature at 303, 313, and 323 K, it is clear from Fig. 10a that the adsorption at 323 K is relatively weakened as compared with that at 303 K and the q_e at 313 K is smaller than that at 303 K.

The fitted q_{max} in Table 6 gives similar results, indicating that a high temperature is unfavorable for the adsorption. Thermodynamic parameters such as the enthalpy change (ΔH, kJ/mol), Gibbs free energy change (ΔG, kJ/mol), and entropy change (ΔS, kJ/(mol K)) can be calculated as [12],

$$\ln K_D = -\frac{\Delta H}{RT} + \ln K_0 \quad (3)$$

$$\Delta G = -RT.\ln K_D \quad (4)$$

$$\Delta S = \frac{\Delta H - \Delta G}{T} \quad (5)$$

where K_D is the distribution coefficient (L/mol) and R is the gas constant (8.303 J/(mol K)). By plotting $\ln K_D$ vs. $1/T$, the ΔH was calculated to be –10.83 kJ/mol (Table 7), clarifying an exothermic process. The negative ΔG indicates that the adsorption is a spontaneous process and the negative ΔS implies a more ordered arrangement of aniline molecules after the adsorption [25].

Additionally, some other amino-containing molecules such as p-aminobenzoic acid and p-phenylenediamine were employed for the equilibrium adsorption, and it can be concluded that the q_e of aniline on 20%-PEDPa is higher than the other two adsorbates (Fig. 10b). The reduced q_e of p-aminobenzoic acid on 20%-PEDPa in comparison of aniline may be from the fact that p-aminobenzoic acid contains carboxyl groups in addition to amino groups, which exists

Table 5
Comparison of the q_{max} of aniline on 20%-PEDPa with some other adsorbents in the literature

	q_{max}/(mg/g)	Reference
Activated kaolinite	256.4 (298 K)	[28]
Natural kaolinite	109.9 (298 K)	[28]
Modified mesoporous silica	17.92 (298 K)	[29]
PHBA-HCLP	184.8 (298 K)	[30]
PS-PH-HCP	178.8 (303 K)	[30]
PAM/SiO_2	52 (293 K)	[42]
HCPs	169 (298 K)	[43]
SA-HCLP	171.2 (298 K)	[44]
20%-PEDPa	163.0 (298 K)	This work

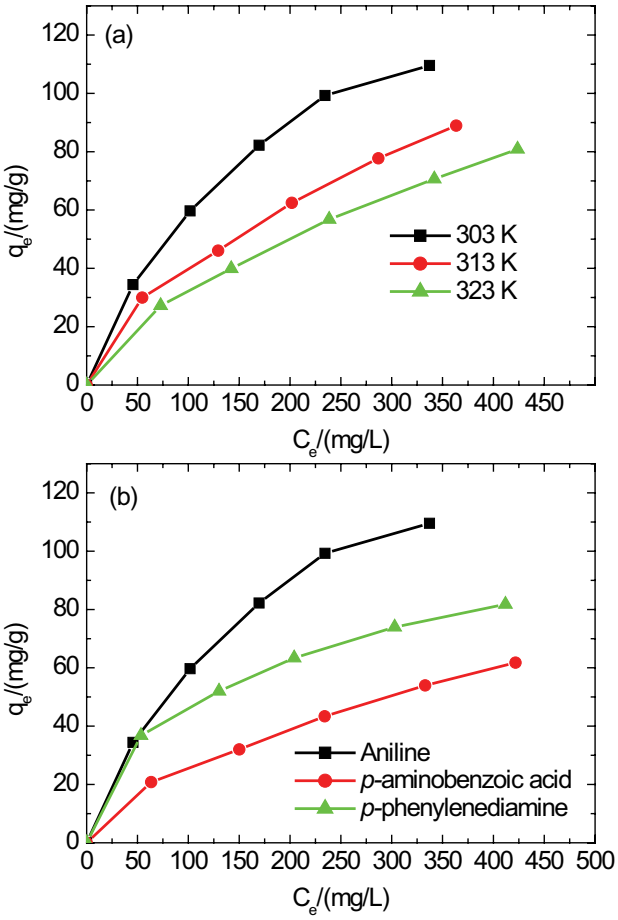

Fig. 10. Equilibrium isotherms of (a) aniline adsorption on 20%-PEDPa at 303, 313, and 323 K and (b) aniline, p-aminobenzoic acid, and p-phenylenediamine on 20%-PEDPa at 303 K.

Table 6
Fitted parameters for the equilibrium data of aniline adsorption on 20%-PEDPa by the Langmuir and Freundlich models

	Langmuir model			Freundlich model		
	K_L (L/g)	q_m (mg/g)	R^2	K_F ((mg/g)(L/mg)$^{1/n}$)	n	R^2
303 K	3.322×10^{-3}	163.0	0.9913	2.583	1.659	0.9981
313 K	3.029×10^{-3}	140.0	0.9794	2.175	1.516	0.9943
323 K	2.124×10^{-3}	121.2	0.9588	1.897	1.486	0.9988

Table 7
Thermodynamics parameters of aniline adsorption on 20%-PEDPa from aqueous solution

ΔH/(kJ/mol)	ΔG/(kJ/mol)			ΔS/(J/(mol K))		
–10.83	303 K	313 K	323 K	303 K	313 K	323 K
	–2.478	–2.472	2.461	–27.57	–26.71	–25.85

electrostatic repulsion with the carboxyl groups of 20%-PEDPa. The relatively low q_e of p-phenylenediamine (47 g/L in water) should be from its higher solubility than aniline (36 g/L in water), and this confirms that the composition and morphology of the polymers are more important in the adsorption than the dendrimers. The effect of the solution pH on the adsorption was recorded in Fig. 11a, and it is seen that the original aniline solution without HCl and NaOH regulation is the most favorable for adsorption. As adding HCl in the solution, the positive ionic form of aniline was the existing form, which is not favorable for the adsorption. On the other hand, the q_e is also decreased as adding NaOH in the solution due to the ionic form of the polymers. Owing to the coexistence of the inorganic salts such as NaCl with the industrial aniline wastewater, the effect of NaCl on the adsorption was determined and the results in Fig. 11b depicts that NaCl exhibits a positive effect on the adsorption. The q_e increases with increasing of the NaCl concentration, which may be from the "salting-out" effect [21]. After the adsorption, the polymers were desorbed by 5% HCl aqueous solution and 20% ethanol, higher than 98.6% aniline was desorbed from the polymers. The polymers were repeated used for six cycles (Fig. 11c), and it is observed that the q_e decreased from 109 mg/g to 101 mg/g with a 7% decreasing ratio, implying that this kind of polymers can be repeated used with excellent regeneration performance.

3.3. Kinetic adsorption

As can be seen from Fig. 12a, the required time for the adsorption of aniline on the polymers from the beginning to the equilibrium is short than 30 min, implying a rapid process. This fast adsorption is important for developing the adsorbent and the hierarchical microporous and mesoporous structure should be the main reason. 10 min is sufficient for the adsorption attaining equilibrium at 323 K, while approximately 20 min is needed at 313 K and 30 min is enough at 303 K, suggesting the adsorption is faster at a higher temperature due to the greater collision rate. Particularly, the final q_e is decreased with increasing the temperature, consistent with the equilibrium experiments. The experimental data were analyzed using pseudo-first-order and pseudo-second-order rate models [45,46]. The relevant parameters are listed in Table 8. The latter is shown to be more appropriate

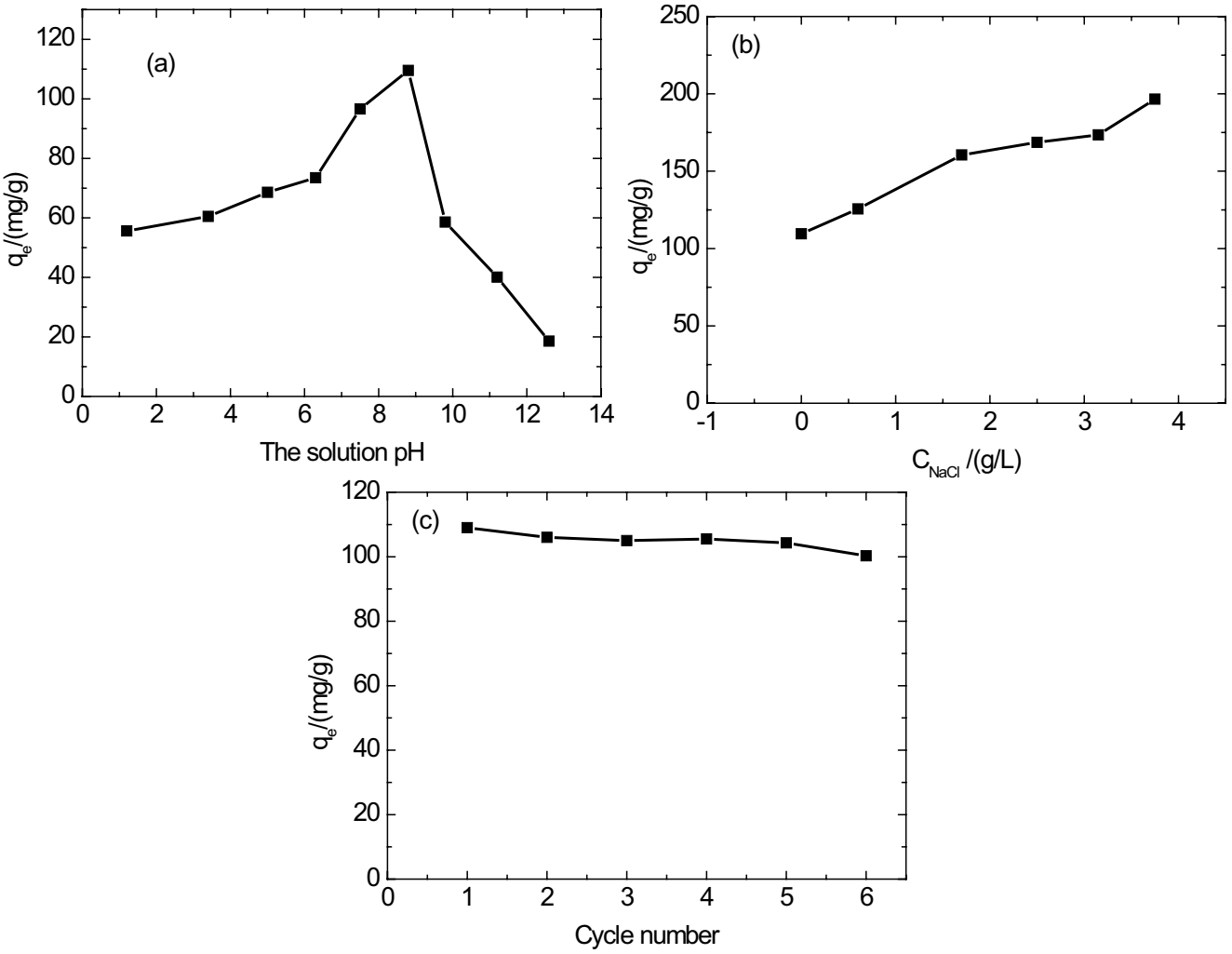

Fig. 11. (a) Effect of the solution pH, (b) NaCl, and (c) repeated use performance on the adsorption of aniline on 20%-PEDPa at 303 K.

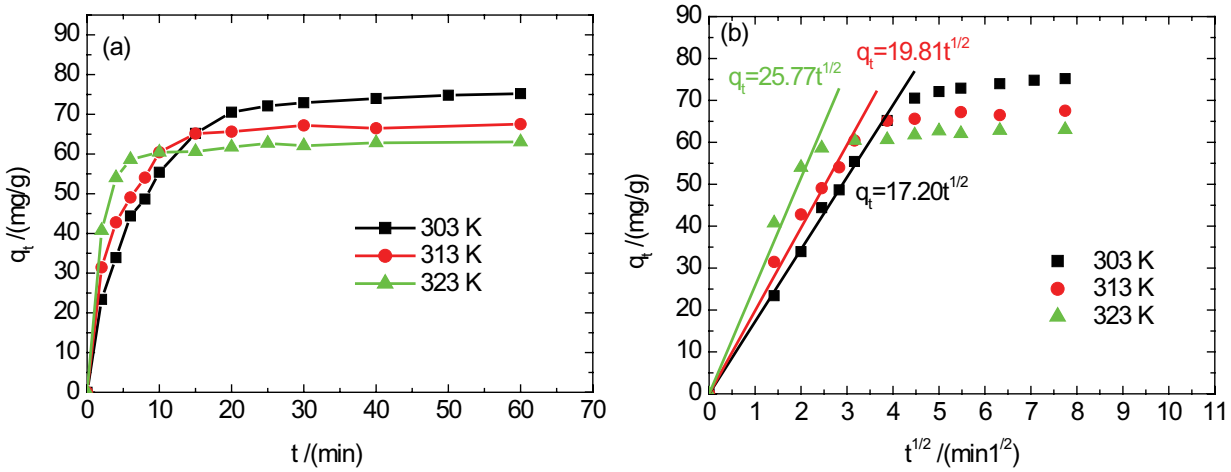

Fig. 12. (a) Kinetic curves of aniline adsorption on 20%-PEDPa from aqueous solution at 303, 313, and 323 K and (b) fitted kinetic curves by a micropore diffusion model.

Table 8
Fitted parameters for the kinetic data of aniline adsorption on 20%-PEDPa from an aqueous solution according to pseudo-first-order and pseudo-second-order rate equations

	Pseudo-first-order			Pseudo-second-order		
	k_1 (min^{-1})	q_e (mg/g)	R^2	k_2 (g/(mg min))	q_e (mg/g)	R^2
303 K	0.1323	73.66	0.9770	1.904×10^{-3}	85.00	0.9997
313 K	0.2526	76.73	0.9626	4.958×10^{-3}	83.41	0.9926
323 K	0.6691	78.82	0.9812	2.291×10^{-2}	80.79	0.9924

for characterizing the kinetic data due to the much higher R^2 (>0.99). Noticeably, the values of k_2 at 303, 313, and 323 K are determined to be 1.904×10^{-3}, 4.958×10^{-3}, and 2.291×10^{-2} g/(mg min), respectively, agrees with the experimental fact that the required time to the equilibrium is shortened as the temperature increases. The intra-particle diffusion model proposed by Weber and Morris was further used to analyze the kinetic data [47],

$$q_t = k_p \times t^{1/2} \tag{6}$$

where k_p is the diffusion parameter ((mg/g)/(min)$^{1/2}$). The fitted results are shown in Fig. 12b, it is discovered that the fitting data is divided into two linear fitting sections with a further horizontal section. In the first linear fitting region, the values of the k_p increase from 17.20 to 19.81 and 25.77 (mg/g)/(min)$^{1/2}$, indicating that the intra-particle diffusion increases with the higher temperature and the intra-particle diffusion step is the rate-controlling step for the adsorption.

4. Conclusions

A series of carboxyl functionalized hyper-cross-linked dendrimers was successfully prepared by four continuous chemical reactions namely polymerization, Friedel–Crafts reaction, amination reaction, and carboxylation reaction. The polymer 10%-PEDPa possessed the highest S_{BET} while the lowest V_{total} with the values of 859 m^2/g and 0.62 cm^3/g, while 40%-PEDPa had the highest uploading carboxyl, amino, and amido groups. The adsorption of aniline on these dendrimers was efficient and the adsorption driving force was mainly based on acid-base interaction, electrostatic interaction, and hydrogen bonding. The adsorption was an exothermic process with the ΔH of –10.83 kJ/mol. 10 min was enough for the adsorption attaining the equilibrium at 323 K due to the hierarchical microporous and mesoporous structure. The kinetic data could be well described by the pseudo-second-order rate model with the k_2 of 2.291×10^{-2} g/(mg min). The intra-particle diffusion model fitted the kinetic data very well with the k_d of 25.77 (mg/g)/(min)$^{1/2}$. The present study gives a new idea for the synthesis of the functionalized hyper-cross-linked dendrimers and this kind of novel polymers have potential application for efficient removal of heavy metals.

Acknowledgment

The National Natural Science Foundation of China (No. 51673216) is gratefully acknowledged for the financial supports.

References

[1] X.X. Yang, Q.X. Guan, W. Li, Effect of template in MCM-41 on the adsorption of aniline from aqueous solution, J. Environ. Manage., 92 (2011) 2939–2943.
[2] H. Yan, H. Wu, K. Li, Y.W. Wang, X. Tao, H. Yang, A.M. Li, R.S. Cheng, Influence of the surface structure of graphene oxide on

the adsorption of aromatic organic compounds from water, ACS Appl. Mater. Interfaces, 7 (2015) 6690–6697.
[3] S. Suresh, V.C. Srivastava, I.M. Mishra, Adsorptive removal of aniline by granular activated carbon from aqueous solutions with catechol and resorcinol, Environ. Sci. Technol. Lett., 33 (2012) 773–781.
[4] J.O. Brien, T.F.O. Dwyer, T. Curtin, A novel process for the removal of aniline from wastewaters, J. Hazard. Mater., 159 (2008) 476–482.
[5] M. Kumar, R. Tamilarasan, Modeling studies: adsorption of aniline blue by using *Prosopis Juliflora* carbon/Ca/alginate polymer composite beads, Carbohydr. Polym., 92 (2013) 2171–2180.
[6] A.A. Gürten, S. Uçan, M.A. Özler, A. Ayar, Removal of aniline from aqueous solution by PVC-CDAE ligand-exchanger, J. Hazard. Mater., 120 (2005) 81–87.
[7] V.A. Davankov, M.P. Tsyurupa, Structure and properties of hypercrosslinked polystyrene-the first representative of a new class of polymer networks, React. Funct. Polym., 13 (1990) 27–42.
[8] M.P. Tsyurupa, V.A. Davankov, Hypercrosslinked polymers: basic principle of preparing the new class of polymeric materials, React. Funct. Polym., 53 (2002) 193–203.
[9] L.S. Shao, M.Q. Liu, Y.F. Sang, J.H. Huang, One-pot synthesis of melamine-based porous polyamides for CO_2 capture, Microporous Mesoporous Mater., 285 (2019) 105–111.
[10] X.M. Wang, H. Ou, J.H. Huang, One-pot synthesis of the hyper-cross-linked polymers chemically modified with pyrrole, furan, and thiophene for phenol adsorption from aqueous solution, J. Colloid Interface Sci., 538 (2019) 499–506.
[11] Z. Liu, F. Zhou, J.H. Huang, Imidazolium salt incorporated poly (N-vinylimidazole-co-ethylene glycol dimethacrylate) for efficient adsorption of congo red and Hg^{2+} from aqueous solution, J. Chem. Eng. Data, 64 (2019) 2627–2633.
[12] F. Zhou, R.L. Man, J.H. Huang, Hyper-cross-linked polymers functionalized with primary amine and its efficient adsorption of salicylic acid from aqueous solution, J. Chem. Thermodyn., 131 (2019) 387–392.
[13] D.A.H. Tomalia, H. Baker, J. Dewald, M. Hall, G. Kallos, S. Margin, J. Roeck, J. Ryder, P. Smith, A new class of polymers: starburst-dendritic macromolecules, Polym. J., 17 (1985) 117–132.
[14] B. Klajnert, M. Bryszewska, Dendrimers: properties and applications, Acta Biochim. Pol., 48 (2001) 199–208.
[15] W.D. Xiao, B. Yan, H.B. Zeng, Q.Q. Liu, Dendrimer function-alized graphene oxide for selenium removal, Carbon, 105 (2016) 655–664.
[16] A. Rether, M. Schuster, Selective separation and recovery of heavy metal ions using water-soluble N-benzoylthiourea modified PAMAM polymers, React. Funct. Polym., 57 (2003) 13–21.
[17] B. Hayati, N.M. Mohammad, M. Arami, F. Mazaheri, Dye removal from colored textile wastewater by poly(propylene imine) dendrimer: operational parameters and isotherm studies, CLEAN Soil Air Water, 39 (2011) 673–679.
[18] A.K. Sharma, A. Gothwal, P. Kesharwani, H. Alsaab, A. Iyer, U. Gupta, Dendrimer nanoarchitectures for cancer diagnosis and anticancer drug delivery, Drug Discovery Today, 22 (2017) 314–326.
[19] J.F. Kukowska-Latallo, K.A. Candido, Z.Y. Cao, S.S. Nigavekar, I.J. Majoros, T.P. Thomas, L.P. Balogh, M.K. Khan, J.J.R. Baker, Nanoparticle targeting of anticancer drug improves therapeutic response in animal model of human epithelial cancer, Cancer Res., 65 (2005) 5317–5324.
[20] C.T. Pang, A.J. Ammit, Y.Q.E. Ong, N.J. Wheate, Para-Sulfonatocalix[4]arene and polyamidoamine dendrimer nano-complexes as delivery vehicles for a novel platinum anticancer agent, J. Inorg. Biochem., 176 (2017) 1–7.
[21] C. Deraedt, R. Ye, W.T. Ralston, F.D. Toste, G.A. Somorjai, Dendrimer-stabilized metal nanoparticles as efficient catalysts for reversible dehydrogenation/ hydrogenation of N-heterocycles, J. Am. Chem. Soc., 139 (2017) 18084–18092.
[22] M. Dodangeh, K. Gharanjig, M. Arami, A novel Ag^+ cation sensor based on polyamidoamine dendrimer modified with 1,8-naphthalimide derivatives, Spectrochim. Acta, Part A, 154 (2016) 207–214.
[23] A.N. Golikand, K. Didehban, L. Irannejad, Synthesis and characterization of triazine-based dendrimers and their application in metal ion adsorption, J. Appl. Polym. Sci., 123 (2011) 1245–1251.
[24] Z.Y. Niu, R.J. Qu, H. Chen, L. Mu, X.Q. Liu, T. Wang, Y. Zhang, C.M. Sun, Synthesis of silica gel supported salicylaldehyde modified PAMAM dendrimers for the effective removal of Hg(II) from aqueous solution, J. Hazard. Mater., 278 (2014) 267–278.
[25] X.M. Yuan, F. Zhou, R.L. Man, J.H. Huang, Dendritic post-cross-linked resin for the adsorption of crystal violet from aqueous solution, J. Chem. Thermodyn., 130 (2019) 235–242.
[26] R.X. Peng, G. Chen, F. Zhou, R.L. Man, J.H. Huang, Catalyst-free synthesis of triazine-based porous organic polymers for Hg^{2+} adsorptive removal from aqueous solution, Chem. Eng. J., 371 (2019) 260–266.
[27] S. Amerkhanova, R. Shlyapov, A. Uali, The active carbons modified by industrial wastes in process of sorption concentration of toxic organic compounds and heavy metals ions, Colloids Surf., A, 532 (2017) 36–40.
[28] Z.J. Liang, W.X. Shi, Z.W. Zhao, T.Y. Sun, F.Y. Cui, Enhanced removal and adsorption characters of aniline by the inorganically modified mesoporous silica nano-spheres, Colloids Surf., A, 513 (2017) 250–258.
[29] H. Koyuncu, A.R. Kul. Removal of aniline from aqueous solution by activated kaolinite: kinetic, equilibrium and thermodynamic studies, Colloids Surf., A, 569 (2019) 59–66.
[30] X.M. Wang, J.L. He, J.H. Huang, Amino-modified hyper-cross-linked polymers with hierarchical porosity for adsorption of salicylic acid from aqueous solution, J. Chem. Thermodyn., 131 (2019) 1–8.
[31] J.R. Caldwell, H.V. Moyer, Determination of chloride: a modification of the Volhard method, Ind. Eng. Chem., 7 (1935) 447–450.
[32] G. Wang, J.R. Wang, H. Zhang, Z. Ling, J.S. Qiu, In situ synthesis of chemically active ZIF coordinated with electrospun fibrous film for heavy metal removal with a high flux, Sep. Purif. Technol., 177 (2016) 257–262.
[33] S.B. Deng, Y.P. Ting, Polyethylenimine-modified fungal biomass as a high-capacity biosorbent for Cr(VI) anions: sorption capacity and uptake mechanisms, Environ. Sci. Technol., 39 (2005) 8490–8496.
[34] H.Y. Shen, S.D. Pan, Y. Zhang, X.L. Huang, H.X. Gong, A new insight on the adsorption mechanism of amino-functionalized nano-Fe_3O_4, magnetic polymers in Cu(II), Cr(VI) co-existing water system, Chem. Eng. J., 183 (2012) 180–191.
[35] Y.J. Shi, T. Zhang, H.Q. Ren, A. Kruse, R.F. Cui, Polyethylene imine modified hydrochar adsorption for chromium (VI) and nickel (II) removal from aqueous solution, Bioresour. Technol., 247 (2018) 370–379.
[36] N. Mao, L.Q. Yang, G.H. Zhao, X.L. Li, Y.F. Li, Adsorption performance and mechanism of Cr(VI) using magnetic PS-EDTA resin from micro-polluted waters, Chem. Eng. J., 200–202 (2012) 480–490.
[37] Y. Zhang, Y.N. Chen, C.Z. Wang, Y.M. Wei, Immobilization of 5-aminopyridine-2-tetrazole on cross-linked polystyrene for the preparation of a new adsorbent to remove heavy metal ions from aqueous solution, J. Hazard. Mater., 276 (2014) 129–137.
[38] S. Zulfiqar, D. Mantione, O. El Tall, M.I. Sarwar, F. Ruiperez, A. Rothenberger, D. Mecerreyes, Nanoporous amide networks based on tetraphenyladamantane for selective CO_2 capture, J. Mater. Chem. A, 4 (2016) 8190–8197.
[39] S.Q. Wang, L.S. Shao, Y.F. Sang, J.H. Huang, Hyper-cross-linked polymers with hollow core-shell structure for efficient Rhodamine B adsorption and CO_2 capture, J. Chem. Eng. Data, 64 (2019) 1662–1670.
[40] I. Langmuir, The constitution and fundamental proprties of solids and liquids, J. Franklin Inst., 184 (1916) 102–105.
[41] H.M.F. Freundlich, Over the adsorption in solution, J. Phys. Chem., 57 (1906) 1100–1107.

[42] F.Q. An, X.Q. Feng, B.J. Gao, Adsorption of aniline from aqueous solution using novel adsorbent PAM/SiO_2, Chem. Eng. J., 151 (2009) 183–187.
[43] Y. Liu, X.L. Fan, X.K. Jia, B.L. Zhang, H.P. Zhang, A.B. Zhang, Q.Y. Zhang, Hypercrosslinked polymers: controlled preparation and effective adsorption of aniline, J. Mater. Sci., 51 (2016) 8579–8592.
[44] Y.Q. Gan, G. Chen, Y.F. Sang, F. Zhou, R.L. Mana, J.H. Huang, Oxygen-rich hyper-cross-linked polymers with hierarchical porosity for aniline adsorption, Chem. Eng. J., 368 (2019) 29–36.
[45] S. Azizian, Kinetic models of sorption: a theoretical analysis, J. Colloid Interface Sci., 276 (2004) 47–52.
[46] Y.S. Ho, G. McKay, Pseudo-second-order model for sorption processes, Process Biochem., 34 (1999) 451–465.
[47] C.M. Sun, R.J. Qu, C.N. Ji, Q. Wang, C.H. Wang, Y.Z. Sun, G.X. Cheng, A chelating resin containing S, N and O atoms: synthesis and adsorption properties for Hg (II), Eur. Polym. J., 42 (2006) 188–194.